sciendo

**Management Systems in Production Engineering**

2020, Volume 28, Issue 4, pp. 298-303

Date of submission of the article to the Editor: 03/2020
Date of acceptance of the article by the Editor: 07/2020

DOI 10.2478/mspe-2020-0042

# GAS FLOW SIMULATION IN THE WORKING GAP OF IMPULSE GAS-BARRIER FACE SEAL

*Eduard KUZNETSOV, Volodymyr NAHORNYI*
*Sumy State University*

*Tibor KRENICKÝ*
*Technical University of Kosice*

**Abstract:**
Numerical simulation method of the working process of a centrifugal unit contactless face impulse seal is proposed. A seal functioning physical model was created. Its operation key aspects that are not taken into account in the traditional methods of calculating contactless impulse seals are identified. A numerical simulation of seal working process based on the Reynolds equation solution for the medium vortex-free motion in the gap between moving surfaces is proposed. Hypothesis that simplify the equation's numerical solution for the face impulse seal is formulated. The numerical solution is obtained using the boundary element method. Based on the obtained numerical solution, the distribution of the working medium pressure field in the seal gap is simulated.

***Key words:*** *impulse gas seal, barrier gas, boundary element method, pressure distribution*

## INTRODUCTION

Currently, double and tandem seals with liquid lubrication are widely used in chemical production equipment, but since late 20 century leading companies have been developing double gas seals designs for pumps and chemical production devices, which in their performance characteristics significantly exceed seals with liquid lubrication [1, 8]. The vast majority of these seals use the gas-dynamic principle of operation by creating a gas-dynamic lifting force with, spiral, logarithmic or other micro-grooves on the working surfaces, that provides a non-contact mode of operation when unit rotor rotates [12, 13]. They are not inferior to the newly developed a contactless gas-barrier face seal design, which uses impulse operation principle (IGBFS) [2, 35]. It does not contain micro-grooves on the working surfaces, and a lubrication film of gas is created and maintained by special feed channels that supply the barrier gas into the operation gap, and isolated chambers that accumulate gas (Fig. 1).

The seal design is simple, compact and due to the impulse principle of creating a gap is able to maintain performance in a wide range of sealing and barrier pressures [14, 15].

The creation of this type new seals is impossible without the development of a theoretical model of its operation process. The basis for the creation of such a model is the analysis of the experimental studies results of the seal function in different modes of operation.

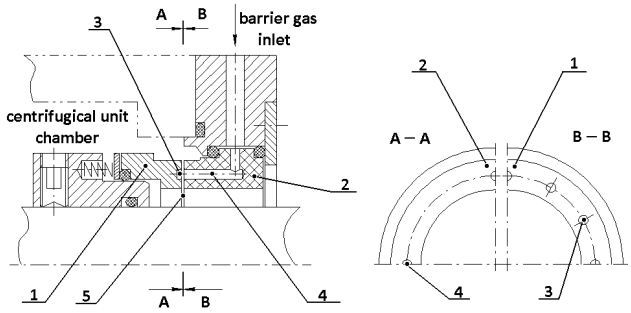


***Fig. 1 Impulse face seal***
***1 – rotated sealing ring with chambers; 2 – fixed mating ring with channels; 3 – isolated chamber; 4 – feed channel; 5 – operation gap***

Main aim of this paper is to provide an analysis-based approach to determining a critical seal characteristic such as pressure distribution in the operation face gap.

## LITERATURE REVIEW

In order to study the function of the seal, a set of experimental studies was carried out. As a result, the flow of barrier gas through the face gap was studied. The studies included measurements of flow rate characteristics and pressure at key locations of the gap [2, 4, 5, 6, 7]. The results of the study of such seals can also be found in the works [17]. The development of a mathematical model is

based on a physical model of operation process that generalizes the analysis of experimental studies [3, 19, 20, 21, 22, 23, 24, 25].

When calculating the IGBFS characteristics, it is usually assumed that the gas pressure in the gap space between the chambers does not differ from some averaged pressure in the chambers [9, 10, 17, 18, 34]. This occurs when the space size between the cameras is commensurate with the circumferential cameras length. However, as shown by recent experimental studies [2, 4, 5, 16], the efficiency and the seal reliability can be significantly increased by changing the number of chambers and feeders, i.e. by changing the inter-chamber spaces [28, 30, 31, 32].

Thus, in order to create more perfect seals, it is necessary to take into account the pressure unevenness factor in the circumferential direction, i.e. the pressure drop in the space between the chambers, when determining the pressure distribution in the seal gap [2, 4, 5, 29].

In this article, we propose a method for determining the pressure distribution in the impulse seal gap, taking into account both the radial gas flow due to the difference between the sealing and atmospheric pressure, and the circumferential flow caused by the sealing surfaces relative rotation [36, 37, 38, 39].

**METHODOLOGY – CALCULATION MODEL SELECTION**

Usually, the Reynolds equation, widely known from the hydrodynamic lubrication theory, is used to calculate the liquid or gas pressure. This equation relates the lubricant pressure function *p(x,z)* (Pa) to its layer thickness *h* (m), its viscosity $\mu$ (Pa·s), density $\rho$ (kg/m$^3$), and working surfaces movement speed *U* (m/s):

$$\frac{\partial}{\partial x}\left(\rho h^3 \frac{\partial p}{\partial x}\right)+\frac{\partial}{\partial z}\left(\rho h^3 \frac{\partial p}{\partial z}\right)=6\mu\frac{\partial(phU)}{\partial x}+12\mu\frac{\partial(ph)}{\partial t}. \quad (1)$$

Water ($\rho = const$) or gas ($\rho \neq const$) can act as a lubricant in this equation. Calculation are performed for the gas lubrication layer. This equation is universal, since it can be used both for calculating bearings (flat, cylindrical, conical, spherical) and for calculating seals (gas-static and gas-dynamic) [4]. The pressure calculation distribution in the IGBFS gap also based on this equation use. Due to the equation non-linearity (1), its analytical integration in general form is currently not possible. In practice, it is possible to obtain quotient solution, but only by a numerous simplifying hypotheses, and when calculating the characteristics, one has to resort to integrating the equation numerical methods using a computer. All of them are based on the transformation equation (1) into a dependence with finite differences, solved by the method of subsequent iterations. The methods are similar and differ only in the boundary conditions that are defined for each specific case. The Raimondi method is the most widely used, which is the most accurate, but has high requirements for computing tools and methods for discretizing solution parcel which is reflected in the convergence of finite difference equations. Therefore, the nomograms available in the literature for determining the gas lubricant layer bearing capacity are intended mainly for support bearings, and for individual eccentricities values and relative sliding surfaces lengths [40].

In most cases, for engineering calculations of hydro- or gas-dynamic units, a stationary one-dimensional lubrication equation is considered, i.e. the lubricating medium pressure or shear flow is neglected [2]. In this case, equation (1) will take the form:

$$\frac{\partial}{\partial x}\left(\rho h^3 \frac{\partial p}{\partial x}\right)=6\mu\frac{\partial(phU)}{\partial x}. \quad (2)$$

For hydrostatic and gas-static units, the right side of equation (2) equals to zero:

$$\frac{\partial}{\partial x}\left(\rho h^3 \frac{\partial p}{\partial x}\right)=0. \quad (3)$$

Equations (2) and (3) have analytical solutions for simple boundary conditions, which are often used to calculate the main of couple sliding characteristics. However, in some cases, the results obtained using this simplified Reynolds equation are not accurate enough. The paper considers the Reynolds equation solution, which is performed by the modern numerical method of boundary elements. This method is quite simple to implement and does not require the method choice for sampling the calculated parcel. By expressing $\rho = p^{\kappa}$ ($\kappa$ – the polytropy index) and assuming, as a first approximation, that the gas flow mode in the gap does not change over time ($\partial p/\partial t = 0$), it is possible to rewrite (1) as:

$$\frac{\partial}{\partial x}\left(h^3 \frac{\partial p^{\left(1+\frac{1}{\kappa}\right)}}{\partial x}\right)+\frac{\partial}{\partial z}\left(h^3 \frac{\partial p^{\left(1+\frac{1}{\kappa}\right)}}{\partial z}\right)=6\left(\frac{1}{\kappa}+1\right)\frac{\partial}{\partial x}\left(Up^{\frac{1}{\kappa}}h\right). \quad (4)$$

Equation (4) is a Poisson equation. To find its solution, you can use the following method [4]: find a solution (1) without the right part (in the form of the Laplace equation), and then subtract a particular solution (the right part) that does not depend on the boundary conditions from the resulting general solution. It is possible to lead (1) to the Laplace equation by assuming that the gas flow mode in the end gap is only radial, i.e., due to the pressure difference between the outer and inner radii of the sealing gap. Then, after introducing a substitution $P = p^{1+1/\kappa}$ that takes into account the lubricant density change when the pressure changes (compressibility of the medium), equation (4) is rewritten as:

$$\frac{\partial}{\partial x}\left(h^3 \frac{\partial P}{\partial x}\right)+\frac{\partial}{\partial z}\left(h^3 \frac{\partial P}{\partial z}\right)=0. \quad (5)$$

Unknown values in this equation are the target pressure function *P* and the value of the gap *h*. The gap value also is a coordinate function in the circumferential direction, and characterized by inclination sealing rings in radial and warping under the action of pressure. The sealing surfaces rotations under pressure, as well as radial and axial forces, can be determined using the well-known Biceno axisymmetric deformations theory. Earlier calculations show that, in the first approximation, it is assumed that *h* is too little changes in the circumferential and radial directions and this change can be ignored. Then the expression (5) will take the Laplace equation form with respect to only the desired pressure function *P*:

$$\frac{\partial^2 P}{\partial x^2}+\frac{\partial^2 P}{\partial z^2}=0\,. \tag{6}$$

Equation (6) describes the gas flow in the IGBFLS end gap. Next, solving method it will be considered.

**RESULTS OF THE NUMERICAL SOLUTION METHOD**

The boundary element method used in this paper is now becoming increasingly popular in continuum mechanics problems [11]. The essence of this method is to reduce the boundary value problem for the partial differential equation (6) to an integral equation along the study parcel (region) boundary, which is obtained by applying the third Green formula to the target function. In general, the integral equation for a region with a boundary has the form:

$$c(\xi)P(\xi)+\int_{\Gamma} P(x)\,q^*(\xi,x)\,d\Gamma(x)=\int_{\Gamma} q(x)\,P^*(\xi,x)\,d\Gamma(x)\,, \tag{7}$$

where:

$\xi$ – is an arbitrary point on the region boundary;

$c(\xi)$ – function, taking into account the peculiarities arising from the border region integration;

$P^*(\xi,x) = (1/2\pi)\cdot ln(1/r)$ – is a fundamental Laplace equation solution for two-dimensional case,

$r$ – the distance between the points $\xi$ and $x$ on the border region (m);

$q^*(\xi,x) = \partial P^*(\xi,x) / \partial n(x)$ (derivative of potential by normal).

The equation solution (7) is carried out by dividing the region boundary into sections (elements), the integration of which is performed numerically by the mechanical Gauss quadrature method. At the next stage of solving the problem, a linear algebraic equations system is obtained, which is solved by the Gauss method. As a result of its solution, unknown values of the function P and $\partial P/\partial n$ on the border are determined, knowing which it is possible to determine the pressure function values at $i$-th point within the region surrounded by the border $\Gamma$:

$$P_i=\int_{\Gamma} q\,P^*\,d\Gamma-\int_{\Gamma} P\,q^*\,d\Gamma\,. \tag{8}$$

Thus, in comparison with the finite difference method, the problem solution becomes less cumbersome, since to determine the pressure distribution field in the region, it is necessary to discretize only the boundary, and not the region itself, which is much easier. In addition, the solution accuracy depends very little on the boundary sampling rate and is very high even with a fairly rough. As a region for determining the gas pressure field, a IGBFS sealing surface section is selected that is bounded by the sealing gap outer and inner radii and radial secants that pass through the middle of the adjacent chambers (Fig. 2).

The pressure function is set as boundary conditions: on the outer radius – the sealing pressure $P_1$, on the inner radius – the atmospheric pressure $P_2$, in the zones of the feed channels – the barrier pressure $P_3$, on the radius – the pressure changes according to the quadratic law (isothermal flow).

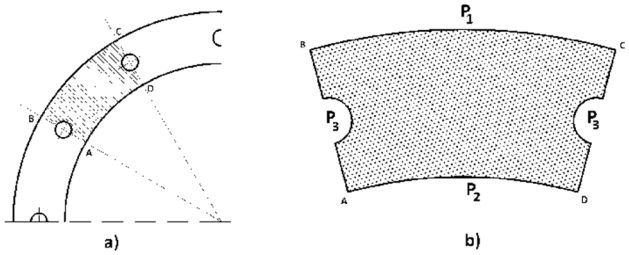


***Fig. 2 Isolation of the region to study the pressure field in the gap between the isolated chambers:***
***a) selection of operation gap sector; b) assigning pressure values at the boundaries of the selected sector***

The integral equation (7) converted to a discrete form by writing it for a number of elements. For the solution, so-called "permanent" elements are used, characterized by the fact that:

a) for each element length, the target function value is set constant;

b) the points where the target function values are considered (nodes) are located in the middle of each element.

The boundary is divided into $N$ elements, each of which has a Dirichlet-type boundary condition (pressure value). Figure 3 shows the outline of the study area divided into elements.

In this case (7) can be written as:

$$c_i P_i+\int_{\Gamma} P\,q^*\,d\Gamma=\int_{\Gamma} q\,P^*\,d\Gamma\,. \tag{9}$$

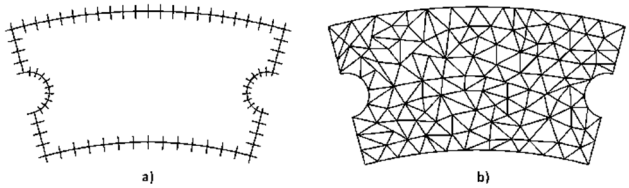


***Fig. 3 Splitting a region boundary and the region itself into elements:***
***a) splitting the sector boundary into separate elements; b) splitting the sector into cells***

Since the Laplace equation for a flat problem is considered and constant elements are used when splitting the boundary, then $P^* = (1/2\pi)\cdot ln(1/r)$ and $c_j = 1/2$. It should be noted that here $\xi$ is taken as the point $i$ for which there is a fundamental solution $P(\xi) = P_i$. For simplicity, the letters $\xi$ and $x$ in parentheses are omitted here. The equation discrete form takes the form:

$$\frac{1}{2}P_i+\sum_{j=1}^{N}\Big(\int_{\Gamma_j} q^*\,d\Gamma\Big)Pu_j=\sum_{j=1}^{N}\Big(\int_{\Gamma_j} P^*\,d\Gamma\Big)q_j\,, \tag{10}$$

where:

$\Gamma_j$ is the length of the $j$-th element.

Integrals $\int_{\Gamma_j} q^*\,d\Gamma$ establish a connection between the $i$-th node and the $j$-th element along the length of which the integral is taken, and will continue to be indicated $H_{ij}$ in the text. Similarly, integrals of the form $\int_{\Gamma_j} P^*\,d\Gamma$ will be

denoted later $G_{ij}$. By entering the designation:

$$H_{ij} = \begin{cases} H_{ij}, & i \neq j \\ H_{ij} + 1/2, & i = j \end{cases}, \quad (11)$$

equation (10) can be written as:

$$\sum_{j=1}^{N} H_{ij} P_j = \sum_{j=1}^{N} G_{ij} q_j . \quad (12)$$

The complete equations system is rewritten in matrix form:

$$HP = GQ . \quad (13)$$

Integrals $H_{ij}$ and $G_{ij}$ are calculated using Gauss quadrature formulas for elements (except for the element to which the node in question corresponds and for which $H_{ij} \equiv 0$ and $G_{ij} = (1/\pi)\cdot(l/2)\ ln(1+1/|l/2|)$ ($l$ – is the element length)). From here, we get an equation that represents the relationship between the inner point $i$ and the values $P$ and $q$ on the border of the region:

$$P_i = \sum_{j=1}^{N} G_{ij} q_j - \sum_{j=1}^{N} \hat{H}_{ij} P_j . \quad (14)$$

Applying (14) to the entire study region with a given step for selecting internal points, it is possible to get an array of values that satisfy equation (6). Finding the right side of equation (4) $W(x) = 6(1+1/\kappa)\ \partial(Uhp^{1/\kappa})/\partial x$ is quite a difficult task. However, it can be solved by successive iterations, substituting the value of the derivative $\partial P/\partial x$ found from (5) into the integral equation (7) in the form:

$$\int_{\Omega} W(x) P^*(\xi, x)\, d\Omega(x) . \quad (15)$$

Here $W(x)$ is taken in region separate points. The derivative $\partial P/\partial x$ is easily determined by the equation:

$$\frac{\partial P(\xi)}{\partial x_i(\xi)} = c(\xi) \int_{\Gamma} q(x) \frac{\partial P^*(\xi, x)}{\partial x_i(\xi)} d\Gamma(x) - \int_{\Gamma} P(x) \frac{\partial q^*(\xi, x)}{\partial x_i(\xi)} d\Gamma(x)] , \quad (16)$$

or using finite difference formulas $(\partial P/\partial x)_i = (P_{i-1}+P_{i+1})/\Delta$. Here $P_{i-1}$ and $P_{i+1}$ is the pressure values at the points $x_{i-1}$ and $x_{i+1}$ in the vicinity of the point $x_i$ (Pa); $\Delta$ – is the distance between the points $x_{i-1}$ and $x_{i+1}$ (m). The value $U$ (m/s) is determined by the rotation speed of the unit rotor, and $h$ (m) in the first approximation is assigned equal to the average value inherent in gas-dynamic seals.

Now, to calculate the integral (15), it is necessary to divide the entire region into separate cells and use numerical integration for them (Figure 3). The complete equations system for $N$ nodes can be represented in matrix form:

$$B + HP = GQ . \quad (17)$$

After finding the values of the functions $P$ and $q$ the entire boundary, it is possible to calculate $P$ at an arbitrary internal point using the expression:

$$P_i = \sum_{j=1}^{N} G_{ij} q_j - \sum_{j=1}^{N} \hat{H}_{ij} P_j - B_i , \quad (18)$$

where:

$B_i$ – is the integral numerical solution (15) for each fundamental solution value given in the $i$-th node.

Applying (14) to the entire study region with a specified step for selecting internal points, obtaining a pressure values field in the impulse seal gap entire sector is possible.

## DISCUSSION

Figure 4 shows examples of calculating the pressure field in the sector between chambers. For the illustrating purpose the pressure distribution, different pressure levels are indicated by different shades of gray. Images a) and c) in the figure correspond to the gap sector with 12 cameras, and images b) and d) correspond to the gap sector with 8 cameras. Sealing rings with a diameter of 80 mm with chambers with a diameter of 3 mm were used. To numerically determine the pressure distribution in the operation gap sector, 50 boundary elements and division of the sector region into 2000 cells were used.

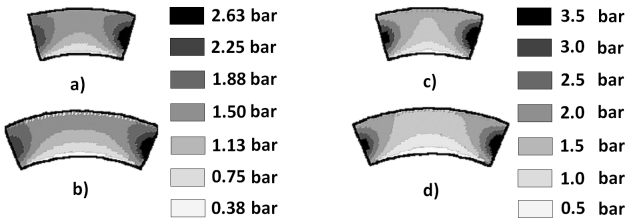


***Fig. 4 Visualization of pressure distribution in the sector of operation gap for seals with 8 and 12 isolated chambers on rotating sealing ring:***
***a) $P_1$ = 2 bar, $P_2$ = 0 bar, $P_3$ = 3 bar, 12 chambers;***
***b) $P_1$ = 2 bar, $P_2$ = 0 bar, $P_3$ = 3 bar, 8 chambers;***
***c) $P_1$ = 1 bar, $P_2$ = 0 bar, $P_3$ = 4 bar, 12 chambers;***
***d) $P_1$ = 1 bar, $P_2$ = 0 bar, $P_3$ = 4 bar, 8 chambers***

The figure clearly shows that the increase in the distance between the chambers (images b and d) is accompanied by an increase in the pressure drop between them. This means that under the same operating conditions with equal gaps, the bearing capacity of the gas lubricant film for a seal with 8 chambers will be less than for a seal with 12 chambers. In other words, other things being equal, a seal with 8 chambers will operate with a face gap smaller than the seal with 12 chambers. Accordingly, the barrier gas flow rate through the seal gap with 8 chambers will be less. This state of affairs is confirmed by experiments: the seal with fewer chambers corresponds to lower flow rates of the gate gas and less sensitivity to changes of the barrier pressure.

## CONCLUSIONS

In this paper, numerical simulation method of the working process of a centrifugal unit contactless face impulse seal is proposed. Firstly, a seal functioning physical model was created and its operation key aspects that are not taken into account in the traditional methods of calculating contactless impulse seals were identified. A numerical simulation of seal working process based on the Reynolds equation solution for the medium vortex-free motion in the gap between moving surfaces were proposed, then the hypothesis that simplify the equation's numerical solution for the face impulse seal was formulated. The numerical solution was obtained using the boundary element method. Based on the obtained numerical solution, the distribution of the working medium pressure field in the seal gap is simulated, revealing dependency between number of the chambers and resulting flow rate.

The presented approach allows to refine the existing method for calculating the gas-barrier impulse seals characteristics by taking into account the irregularity the pressure field in the operation gap in the circumferential direction.

Finally, it should be noted that present method does not take into account the change in gap caused by warping and inclination of the working surfaces. Therefore, the main task of further studies of impulse type gas face seals should consider to clarify the obtained mathematical model.

**ACKNOWLEDGMENTS**

*The authors would like to thank the VEGA grant agency for supporting presented research work within the project VEGA 1/0205/19.*

**REFERENCES**

[1] A. Panda, J. Duplak, J. Jurko and M. Behun. "Comprehensive Identification of Sintered Carbide Durability in Machining Process of Bearings Steel 100CrMn6". *Advanced Materials Research*, vol. 340, pp. 30-33, 2011.

[2] E.G. Kuznetsov and A.E. Chernov. "Study of flow rate characteristics of the impulse gas barrier face seal". *Bulletin of Sumy State University: Engeneering scienses*, vol. 42, pp. 55-60, 2002.

[3] E.G. Kuznetsov. "Determination of pressure field in lubricating layer of pulse-type gas barrier seal". *Printing technology and techniques*, vol. 4(6), pp.78-85, 2004.

[4] E.G. Kuznetsov. "Theoretical and experimental studies of gas barrier impulse mechanical seal". *In: 11th International Scientific and Engineering Conference on Hermetic Sealing, Vibration Reliability and Ecological Safety of Pump and Compressor Machinery, HERVICON 2005*, vol. 11, pp. 156-164, 2005.

[5] E. Kuznetsov, V. Nahornyi, S. Vashchenko, O. Aleksenko, I. Baranova, A. Panda and I. Pandova. "Experimental researches of the pulse gas barrier face seal". *Modern Machinery (MM) Science Journal*, vol. 4, pp. 3519-3522, 2019.

[6] E. Kuznetsov. "Experimental studies of the pressure field in the face gap of the impulse gas-barrier seal". *Impact vibration systems, machines and technologies: materials of the IV International Scientific Symposium.* pp. 50-54, 2010.

[7] E.G. Kuznetsov, L.A. Savin. "Investigation of flow rate characteristics of impulse seal gap". *Bulletin of OryolGTU*, vol. 5(283), pp. 9-13, 2010.

[8] I. Leššo, P. Flegner, M. Šujanský, E. Špak. Research of the possibility of application of vector quantisation method for effective process control of rock desintegration by rotary drilling. *Metalurgija*, vol. 49, pp. 61-65, 2010.

[9] V. Martsynkovskyy, P.N. Vorona. Pumps of nuclear power plants. Energoatomizdat, 256 p., 1987.

[10] V. Martsynkovskyy, A. Zahorulko, S. Gudkov and S. Mischenko. Analysis of buffer impulse seal. *In: 13th International Scientific and Engineering Conference on Hermetic Sealing, Vibration Reliability and Ecological Safety of Pump and Compressor Machinery, HERVICON 2011, vol. 13*, pp. 43-50, 2011.

[11] A. Panda, K. Dyadyura, J. Valicek, M. Harnicarova, J. Zajac, V. Modrak, I. Pandova, P. Vrabel, E. Novakova-Marcincinova and Z. Pavelek. "Manufacturing Technology of Composite Materials – Principles of Modification of Polymer Composite Materials Technology Based on Polytetrafluoroethylene". *Materials,* vol. 10, no. 4, pp. 337, 2017.

[12] J. Valicek, M. Harnicarova, A. Panda, I. Hlavaty, M. Kusnerova, H. Tozan, M. Yagimli and V. Vaclavik. "Mechanism of Creating the Topography of an Abrasive Water Jet Cut Surface". *Machining, joining and modifications of advanced materials*, vol. 61, pp. 111-120, 2016.

[13] A. Panda, Š. Olejárová, J. Valíček and M. Harničárová. "Monitoring of the condition of turning machine bearing housing through vibrations". *International Journal of Advanced Manufacturing Technology*, vol. 97, no. 1-4, pp. 401-411, 2018.

[14] M. Pustan, O. Belcin and B. Corina. Mechanical seals with oscillating stator. *Meccanica*, vol. 48, pp. 1191-1200, 2013.

[15] J. Valicek, M. Harnicarova, I. Kopal, Z. Palková, M. Kušnerová, A. Panda and V. Šepelák. "Identification of Upper and Lower Level Yield strength in Materials". *Materials,* vol. 10, no. 9, pp. 1-20, 2017.

[16] V. Tarelnyk, V.S. Martsinkovskii and A.N. Zhukov. Increase in the Reliability and Durability of Metal Impulse Seals. Part 1. *Chemical and Petroleum Engineering*, vol. 53, pp. 114-120, 2017.

[17] A. Zahorulko. Theoretical and experimental investigations of face buffer impulse seals with discrete supplying. *Eastern-European Journal of Enterprise Technologies*, vol. 4, pp. 45-52, 2015.

[18] A. Zahorulko, D. Lisovenko and V. Martsynkovskyi. Development and investigation of face buffer impulse seal of centrifugal compressor. *Eastern-European Journal of Enterprise Technologies*, vol. 1, pp. 30-39, 2016.

[19] A. Panda, J. Dobránsky, M. Jančík, I. Pandová and M. Kačalová. "Advantages and effectiveness of the powder metallurgy in manufacturing technologies". *Metalurgija*, vol. 57, no. 4, pp. 353-356, 2018.

[20] J. Valicek, M. Harnicarova, I. Hlavaty, R. Grznárik, M. Kusnerova, Z. Mitaľová and A. Panda. "A new approach for the determination of technological parameters for hydroabrasive cutting of materials". *Materialwissenschaft und Werkstofftechnik*, vol. 47, pp. 462-471, 2016.

[21] I. Pandova, T. Gondova and K. Dubayova. "Natural and Modified Clinoptilolite Testing for Reduction of Harmful Substance in Manufacturing Exploitation". *Advanced Materials Research*, vols. 518-523, pp. 1757-1760, 2012.

[22] J. Macala, I. Pandova, T. Gondova and K. Dubayova. "Reduction of polycyclic aromatic hydrocarbons and nitrogen monooxide in combustion engine exhaust gases by clinoptilolite". *Gospodarka Surowcami Mineralnymi*, vol. 28, no. 2, pp. 113-123. 2012.

[23] J. Macala, I. Pandova and A. Panda. "Zeolite as a prospective material for the purification of automobile exhaust gases". *Mineral resources management*, vol. 33, no. 1, pp. 125-138. 2017.

[24] J. Macala, I. Pandova and A. Panda. "Zeolite as a prospective material for the purification of automobile exhaust gases". *Mineral resources management*, vol. 25, no. 4, pp. 23-32. 2009.

[25] A. Panda, V. Nahornyi, I. Pandová, M. Harničárová, M. Kušnerová, J. Valíček and J. Kmec. "Development of the method for predicting the resource of mechanical systems". *International Journal of Advanced Manufacturing Technology*, vol. 105, no. 1-4, pp. 1563-1571, 2019.

[26] M. Balara, D. Duplakova and D. Matiskova. "Application of a signal averaging device in robotics 2018". Measurement. vol. 115, pp. 125-132, 2018.

[27] M. Durdan, B. Stehlikova, M. Pastor, J. Kacur, M. Laciak and P. Flegner. "Research of annealing process in laboratory conditions". *Measurement,* vol. 73, 2015, pp. 607-618. ISSN 0263-2241.

[28] K. Monkova and P. Monka. "Some aspects influencing roduction of porous structures with complex shapes of cells". *Lecture Notes in Mechanical Engineering*, pp. 267-276, 2017.

[29] S. Olejarova, J. Dobransky, J. Svetlik and M. Pituk. "Measurements and evaluation of measurements of vibrations in steel milling process". *Measurement,* vol. 106, pp. 18-25, 2017. ISSN 0263-2241.

[30] M. Rimar, M. Fedak, A. Kulikov and P. Smeringai. "Study of gaseous flows in closed area with forced ventilation." *MM Science Journal*, vol. 2018, no. March, pp. 2188-2191, 2018.

[31] M. Pollák, J. Torok, J. Zajac, M. Kočiško and M. Teliskova. "The structural design of 3D print head and execution of printing via the robotic arm ABB IRB 140". *ICIEA 2018,* vol. 2018, pp. 194-198, 2018.

[32] W. Bialy and J. Ružbarský. "Breakdown cause and effect analysis. Case study". *Management Systems in Production Engineering,* vol. 26, pp. 83-87, 2018.

[33] D. Duplakova, L. Knapcikova, M. Hatala and E. Szilagyi. "Mathematical modelling of temperature characteristics of RFID tags with their subsequent application in engineering production". *TEM Journal-Technology Education Management Informatics,* vol. 5, pp. 411-416, 2016.

[34] J. Kascak, P. Baron, M. Teliskova, J. Zajac, J. Torok and J. Husar. "Implementation of augmented reality into the training and educational process in order to support spatial perception in technical documentation". *6th IEEE international conference on industrial engineering and applications,* pp. 583-587, 2019.

[35] R. Bielousova. "Developing materials for english for specific purposes online course within the blended learning concept". *TEM Journal-Technology Education Management Informatics,* vol. 6, pp. 637-642, 2017.

[36] Ľ. Straka, I. Čorný and J. Piteľ. "Properties evaluation of thin microhardened surface layer of tool steel after wire EDM". *Metals,* vol. 6, no. 5, pp. 1-16, 2016.

[37] Ľ. Straka, I. Čorný and J. Piteľ. "Prediction of the geometrical accuracy of the machined surface of the tool steel EN X30WCrV9-3 after electrical discharge machining with CuZn37 wire electrode". *Metals,* vol. 7, no. 11, pp. 1-19, 2017.

[38] J. Dobránsky, M. Pollák and Z. Doboš. "Assessment of production process capability in the serial production of components for the automotive industry". *Management Systems in Production Engineering,* vol. 27, no. 4, pp. 255-258, 2019.

[39] Ľ. Straka, G. Dittrich. "Influence of graphite tool electrode shape on TWR and MRR at EDM". *MM Science Journal*, vol. 2019, pp. 3479-3485, 2019.

[40] P. Cacko and T. Krenicky. "Impact of lubrication interval to operating status of bearing". *Applied Mechanics and Materials*, vol. 616, pp. 151-158, 2014. ISSN 1660-9336.

**Eduard Kuznetsov**
ORCID ID: 0000-0003-4127-4553
Sumy State University
Faculty of Electronics and Information Technologies
2, Rymskogo-Korsakova st., 40007 Sumy, Ukraine
e-mail: v.nahornyi@cs.sumdu.edu.ua

**Volodymyr Nahornyi**
ORCID ID: 0000-0001-5223-7219
Sumy State University
Faculty of Electronics and Information Technologies
2, Rymskogo-Korsakova st., 40007 Sumy, Ukraine

**Tibor Krenický**
ORCID ID: 0000-0002-0242-2704
Technical University of Kosice
Faculty of Manufacturing Technologies
Sturova 31, 08001 Presov, Slovak Republic
e-mail: tibor.krenicky@tuke.sk